Received: 6 December 2021 | Revised: 11 March 2022 | Accepted: 18 March 2022

DOI: 10.1002/er.7909

SHORT COMMUNICATION

INTERNATIONAL JOURNAL OF ENERGY RESEARCH WILEY

Microstructure and mechanical properties of electrochemically cycled ice-templated $Li_4Ti_5O_{12}$ sintered anodes

Rohan Parai[1] | Ziyang Nie[2] | Dipankar Ghosh[1] | Gary M. Koenig Jr[2]

[1]Department of Mechanical and Aerospace Engineering, Old Dominion University, Norfolk, Virginia, USA

[2]Department of Chemical Engineering, University of Virginia, Charlottesville, Virginia, USA

Correspondence
Gary M. Koenig Jr, Department of Chemical Engineering, University of Virginia, Charlottesville, VA 22904, USA.
Email: gary.koenig@virginia.edu

Dipankar Ghosh, Department of Mechanical and Aerospace Engineering, Old Dominion University, Norfolk, VA 23529, USA.
Email: dghosh@odu.edu

Funding information
National Science Foundation, Grant/Award Number: CMMI-1825216

Summary

In the development of materials to meet increasing demands for energy storage, complex materials and systems will need to be investigated. One emerging area is multifunctional energy storage materials, where a battery electrode needs to satisfy other properties in addition to those associated with storing electrochemical energy. An example explored in this report is sintered electrodes for lithium-ion batteries, where the electrode is only comprised of a porous sintered structure of the electroactive ceramic material. The sintered electrode must be multifunctional in that the porous ceramic itself must sustain the compressive mechanical stresses involved in fabricating the battery cell, as well as the stresses that result during electrochemical charge and discharge cycles. Toward meeting these multifunctional demands, anodes were fabricated using an ice-templating technique, resulting in directionally porous materials. This study reports the microstructure and compressive mechanical properties of an ice-templated sintered electrode material both before and after electrochemical cycling, revealing whether electrochemical cycling affects the microstructure and strength. For the specific electroactive material investigated as ice-templated sintered anodes, the strain with electrochemical cycling was known to be minimal, and the microstructure and compressive strength were found to be retained after multiple charge and discharge cycles. These results suggest multifunctional ice-templated lithium-ion battery electrodes can be produced with both high strength and high cell level energy density.

Novelty Statement

Ice-templated sintered electrodes are multifunctional battery materials with desirable mechanical and electrochemical properties provided by their unique directionally aligned porous microstructure. This is the first study of these thick and high-energy electrodes to report mechanical properties both before and after cycling. Microstructure and mechanical properties were retained after electrochemical cycling, suggesting that at least for relatively low strain

materials that ice-templated sintered electrodes are mechanically robust to strain induced by charge/discharge cycling.

KEYWORDS

ice-templating, lithium-ion battery, mechanical characterization, microstructure, multifunctional porous ceramics, sintered electrode

1 | INTRODUCTION

Lithium-ion batteries (LIBs) conventionally contain composite electrodes, which include conductive additives and polymer binders mixed with solid active material particles.[1] The inactive components provide desired electrode properties including mechanical integrity, flexibility, and electronic conductivity. However, inactive materials reduce the energy density.[2] Inactive additives also have negative consequences on electrochemical properties, including reducing the effective electroactive area and greatly increasing ion transport restrictions.[3,4] Toward overcoming these challenges, researchers have reported electrodes free of inactive materials. One option includes the use of "sintered electrodes," where active material powder is processed and then thermally treated to remove any binders.[5-7] Even for mild thermal treatments, the sintering step improves mechanical stability of the sintered electrode. Sintered electrodes both eliminate inactive additives from the electrode and enable high thicknesses/loading, which increases energy density at the cell level in LIBs.[5,8]

Sintered electrodes have unique advantages over composite electrodes. First, as will be described in this manuscript, they can be fabricated very thick while still maintaining mechanical stability. The thicknesses can even exceed 1000 μm, where at such thicknesses, composite electrodes can be challenging to fabricate with robust mechanical properties via conventional routes.[9,10] Increased thickness for battery electrodes is a general strategy to increase the cell level energy density because less volume and mass are dedicated to inactive current collectors and separators.[11,12] Thus, thick sintered electrodes can result in high energy density at the cell level.[5] A limitation at such great thicknesses will always be the substantive ion and electron transport pathways through the electrode microstructure resulting in ionic and electronic cell overpotentials.[13] For an equivalent thickness, the absence of inactive components for sintered electrodes has the added benefit of eliminating additional materials from the interstitial regions of the electrode microstructure, which means that relative to composite electrodes sintered electrodes do not have material besides the liquid electrolyte in the porous microstructure to further impede lithium ion transport.[1,5,8,14-17] Thus, sintered electrodes in general provide ion transport advantages by eliminating inactive electrode components. In addition, ice-templating further aligns the electrolyte-laden pore regions, which can further enhance effective electrode transport properties.[1,18-20] Sintered electrodes, and more specifically ice-templated sintered electrodes, thus have promise in facilitating multifunctional improvements in LIB electrode energy density and relative transport properties.

In aiming to improve LIB performance, electrode mechanical strength is also important. Electrodes must withstand stresses resulting from the cell assembly process, internal compression which facilitates holding electrodes in appropriate locations, and stresses that originate during electrochemical cycling.[21,22] Failure to sustain these stresses can cause cracking in electrodes and delamination from current collectors, leading to reductions in accessible battery energy, power density, round trip efficiency, and lifetime.[23-25] Sintered electrodes must satisfy the multifunctional role of meeting both electrochemical and mechanical demands of the brittle porous thin film of active material. This results in considering both the electrochemical and mechanical properties of the electrode during the earliest stages, and information is needed on relevant process–property coupling.[26-29] As an example, both energy density and mechanical strength of sintered electrodes can be enhanced by reducing electrode porosity.[30] However, reduction in porosity increases pore tortuosity,[31] enhancing resistance to ion transport through the electrode microstructure and reducing capacity delivered at increased rates and round-trip efficiency.[32,33]

To meet the multifunctional demands of sintered electrodes, ice-templated materials with aligned pore channels and low pore tortuosity have been investigated.[34,35] The directional porosity from ice-templating is desirable for improving effective electrolyte transport properties via reduced pore tortuosity. For ice-templated sintered electrodes, improvements in Li^+ transport, rate capability, and areal capacity have been reported.[34,35] The authors recently investigated electrochemical performance and compressive mechanical properties of ice-templated sintered lithium titanate (LTO, chemical

composition $Li_4Ti_5O_{12}$) anode materials.[1,15,36] LTO is a well-established anode material in LIBs and considered as a "zero-strain" material, with minimal volume change during cycling.[37] Increased rate capability of cells containing ice-templated LTO anodes has been attributed to improved Li^+ transport.[1,15]

There have been few studies on mechanical properties of ice-templated-sintered electrodes.[35] However, investigations on other oxide ceramic materials suggest that another benefit is that at comparable levels of porosity, ice-templated materials exhibit higher compressive strength compared to conventional open-cell foams.[38] With decreasing porosity, the strength difference between sintered templated and non-templated porous ceramics increases. Microstructural features that govern compressive strength of ice-templated ceramics are the presence of lamellar bridges between adjacent lamella walls, where significant strength increases can occur with increased bridge density.[39] Bridge density can be modulated by controlling freezing front velocity (FFV), particle size, particle anisotropy, and additive concentrations.[39-41] The authors have used sucrose (water-soluble additive) to fabricate ice-templated sintered LTO materials, which increased the bridge density and enhanced compressive strength.[32] Other options for strength enhancement include the use of magnetic and electric fields.[42,43]

While the research described above suggests promising electrochemical properties and mechanisms to improve mechanical properties of ice-templated multifunctional electrodes, the influence of electrochemical cycling on the mechanical properties of sintered electrodes has not yet been investigated. In this initial study of cycling influences on the microstructure and mechanical properties of sintered electrodes, LTO was chosen as the anode material, which would be expected to retain mechanical properties due to its minimal volume change during electrochemical cycling.[44] Herein, the uniaxial compressive response of ice-templated-sintered LTO anodes before and after multiple electrochemical cycles will be described. As will be revealed, at least for the first few cycles, characterization of both the microstructure and compressive response from recovered LTO anodes suggested that the electrodes were intact both structurally and mechanically.

2 | EXPERIMENTAL

Experimental details can be found in Sections S.1.1-S.1.5, Figures S1 and S2, and References 34-37. $LiCoO_2$ (LCO) was used as the cathode material, and the detailed process for its synthesis can be found in previous reports.[45] LTO powder (NANOMYTE BE-10 from NEI Corporation) was purchased for use as the anode material, and the powder was not modified or treated before processing for ice-templating. The detailed materials characterization and electrochemical properties of both LCO and LTO materials used in this study can be found in previous publications.[45,46]

For ice-templating, a custom-made device was used, and details of the device can be found elsewhere.[47] Details on fabrication of the ice-templated LTO electrodes can also be found in Section S.1.2. Using this ice-templating device, a total of 12 samples were fabricated in 3 batches at average FFV of $21.9 \pm 0.9\ \mu m\ s^{-1}$. Details on procedures for porosity measurements, microstructural characterization, and mechanical testing of the ice-templated LTO materials can be found in Section S.1.3. Compared to the received LTO powder, there were no noticeable changes in the XRD patterns for ice-templated LTO pellets after thermal processing (patterns can be found in Figure S3). This outcome indicated no changes in the bulk crystal structure during processing and fabrication of the electrode pellets. The XRD patterns were consistent with spinel phase LTO battery electrode materials.[46] Brunauer-Emmett-Teller (BET) surface area of ice-templated LTO was measured to be below $1\ m^2\ g^{-1}$, with higher precision difficult to obtain due to the low total volume of gas adsorbed on the material.[1]

For electrochemical experiments, the ice-templated LTO anodes were paired with sintered LCO cathodes (nontemplated). Preparation of sintered LCO cathodes has been described in previous reports,[5] and additional details can also be found in Section S.1.4. Details for fabrication and electrochemical evaluation of the LTO/LCO full cells can also be found in Section S.1.5. It is noted that the areal active material loading for these electrodes was relatively high for LIB electrodes, where for the LTO electrode, the loading was $0.34\ g\ cm^{-2}$. Assuming ~175 mAh g^{-1} LTO available capacity, there was 59.5 mAh cm^{-2} available in the LTO electrode. Such high capacity limits the ability to cycle such electrodes in lithium metal half cells, as the excessive stripping and plating of the lithium metal consumes electrolyte and causes the cells to fail after limited number of cycles.[5] For example, to cycle an electrode with 59.5 mAh cm^{-2} loading, ~435 μm Li metal needs to be stripped and plated, and it is challenging to suppress the dendrite formation and electrolyte degradation during this process.

3 | RESULTS AND DISCUSSION

3.1 | Electrochemical cycling

The ice-templated-sintered LTO pellets were paired with nontemplated sintered LCO pellets for electrochemical

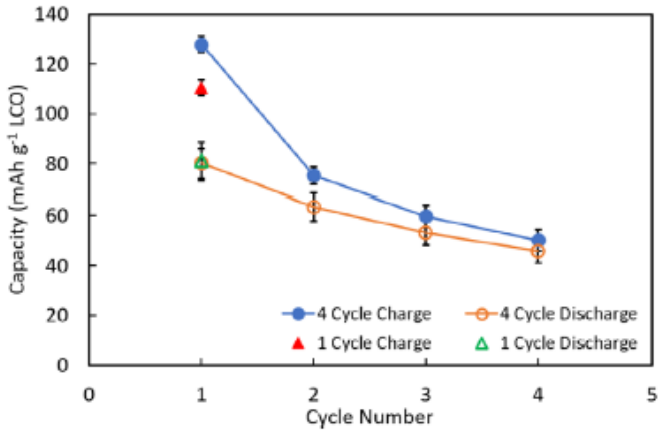

FIGURE 1 Charge and discharge capacity on an $LiCoO_2$ (LCO) gravimetric basis for cells with lithium titanate (LTO) anodes where the LTO/LCO-sintered electrode cells were cycled at C/50. C/50 corresponded to ~1.3 mA (~1.0 mA cm^{-2}). Error bars represent the standard deviations for 5 nominally identical and independently fabricated cells. The outcomes are for the initial charge (red triangle) and discharge (green triangle) for cells cycled a single time, and each charge (blue circle) and discharge (orange circle) for cells cycled 4 times. The voltage limits were 1.0 to 2.8 V (cell)

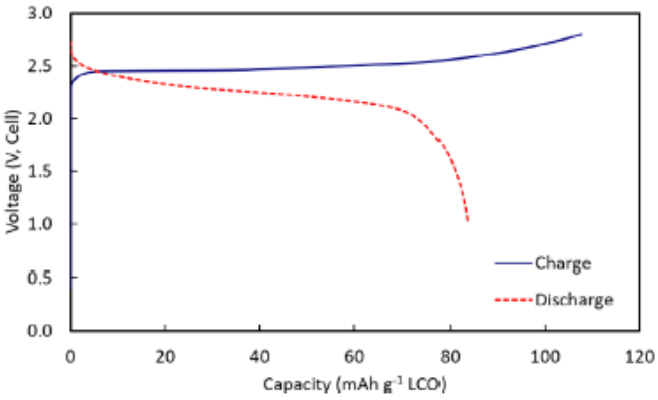

FIGURE 2 Representative initial charge (blue) and discharge (red) polarization curves for a lithium titanate (LTO) anode paired with a $LiCoO_2$ (LCO) cathode for a LTO/LCO sintered electrode cell cycled at a rate of C/50. The voltage limits were 1.0 to 2.8 V (cell)

characterization. The average charge and discharge gravimetric capacity on an LCO basis for 5 nominally identical cells that were cycled for either one or four charge/discharge cycles can be found in Figure 1, which revealed a loss of capacity during the first four cycles. This is not expected to have resulted from intrinsic limitations for LTO/LCO-sintered electrode cells, as cells with similar construction (but much thinner electrodes) have been cycled for hundreds of cycles with much less capacity fade.[5,15] Detailed rate capability has also been reported for cells with sintered LTO anodes, where the LTO electrodes were fabricated via both compression and ice-templated processing.[1,15] However, the specific goal of evaluating mechanical properties of the electrodes after charge/discharge cycling resulted in experimental system compromises that were very different from those prior studies with extended cycling. First, to achieve reliable mechanical compression measurements, pellets at least 2 mm thick were desired, thus the LTO electrodes evaluated were 2 mm thick. At such great thicknesses, the ion transport was restrictive in the cell due to the extended path lengths, even with the ice-templated aligned open pores.[9] The charge and discharge current applied was ~1.3 mA, corresponding to ~1.0 mA cm^{-2} (C/50 based on the LCO gravimetric capacity assumptions). The resulting first discharge gravimetric capacity of LCO was ~64% of that for LCO-sintered electrodes identically synthesized and processed but which were thinner and in sealed coin cells.[15] To achieve higher utilization, slower cycling rates could have been implemented; however, flat cells were challenging to seal. At the end of the four-cycle experiments (which took ~180 hours to complete), electrolyte was observed to have evaporated, and this loss was suspected to be in large part responsible for capacity fade. The cells represented a balance between cycling time limitations for flat cells while using electrodes thick enough for mechanical property evaluation and extents of lithium intercalation/deintercalation such that the material had experienced strain from the associated structural changes.

Typical charge and discharge curves are shown in Figure 2. For comparison, the 1st and the 4th cycles of the cell with multiple cycles can be found in Figure S4. The shape of the curves was consistent with previous reports for sintered LTO/LCO full cells.[1,15] Compared to those prior reports which used thinner LTO/LCO sintered pellets in crimped coin cells, the first charge and discharge gravimetric capacities were lower, which was attributed to the higher electronic and ionic transport resistance for the much thicker pellets used. The average potential of charge/discharge also supported increased resistance for the thicker electrodes. In Figure 2, the average charge potential was ~2.5 V, and the average discharge potential was ~2.2 V. However, in previous work with thinner sintered electrodes in LTO/LCO full cells, the average charge/discharge potentials were both at ~2.4 V at C/50.[1,15] Also, the first cycle columbic efficiency for the flat cell was 78%, while the prior values for thinner electrodes was 87%. This may have in part been caused by more electrode material in the flat cell system resulting in more electrolyte decomposition at the active material interface, especially on the LCO cathode.[15]

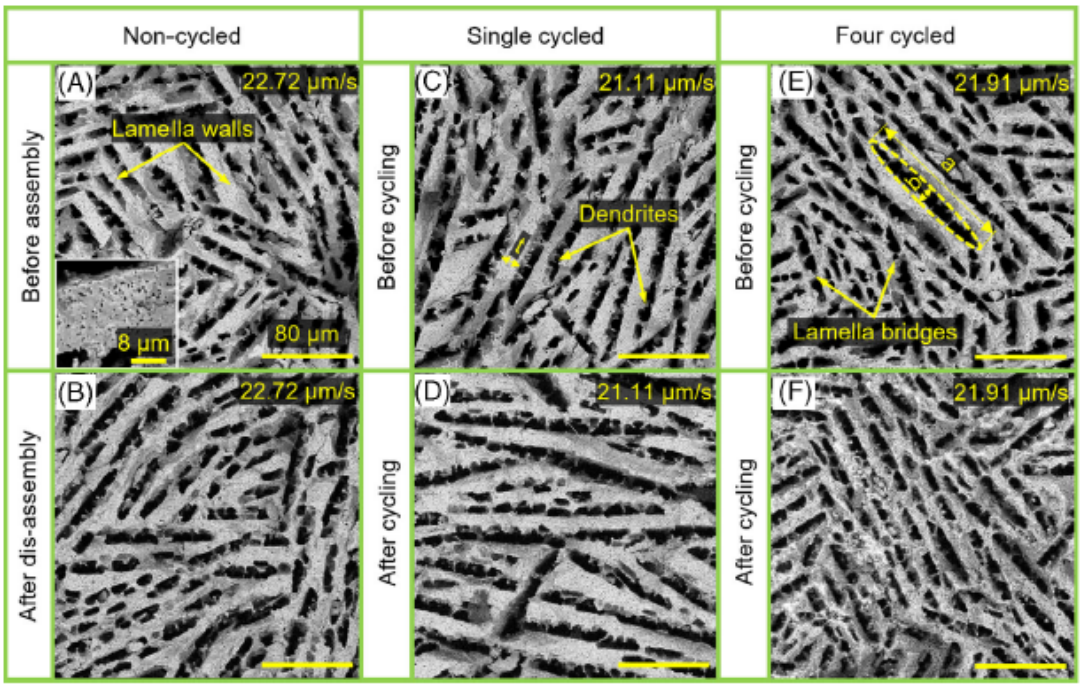

FIGURE 3 Scanning electrode microscopy (SEM) images of noncycled lithium titanate (LTO) ice-templated anodes (A) before assembly and (B) after disassembly in flat cells paired with $LiCoO_2$ (LCO) cathodes. Inset in (A) shows higher magnification image of LTO lamella wall. Microstructure of single-cycled LTO anode (C) before and (D) after cycling. Similarly, microstructure of four-cycled LTO anode (E) before and (F) after cycling

3.2 | Ice-templated LTO microstructure

SEM images in Figure 3 reveal microstructures of ice-templated-sintered LTO anodes before and after electrochemical cycling. Higher magnification SEMs can also be found in Figure S5. These images correspond to the image plane perpendicular to the growth direction of ice crystals. Figure 3A,C,E show SEM images of LTO anodes before electrochemical cycling. The SEM images revealed the characteristic ice-templated microstructure with directional pores that enable efficient ion pathways in the direction of Li^+ net flux. Lamella walls were observed to be porous, containing ultrafine pores (see inset in Figure 3A for a higher magnification SEM image of a wall). Average lamella wall thickness was 16.9 ± 3.6 μm, and the average pore major axis and minor axis were 133.9 ± 36.7 μm and 15.9 ± 2.6 μm, respectively. The errors represent the SD of a minimum of 120 measurements from the SEM images of 3 independent samples. Some of the dendrites on lamella walls were observed to be connected to adjacent walls, resulting in lamellar bridges, as indicated in Figure 3E. As discussed before, lamellar bridges are important for the compressive strength of ice-templated ceramics, as strength increases with bridge density.[39] A previous study by the authors on ice-templated-sintered LTO materials indicated that compressive strength increased with bridge density, and the bridge density was enhanced by the addition of sucrose.[36] Hence, in this work, a relatively high sucrose content (6 wt%) was used with the aim to increase density of lamellar bridges and compressive strength.

Figure 3B is an SEM image of the microstructure of a noncycled LTO anode, where the anode was removed after flat cell assembly but without any electrochemical cycling. After removal, the LTO anode was physically intact, and microscopy did not reveal any cracks/fracture within the anode. Therefore, from comparison of Figure 3A,B, it was concluded that flat cell assembly and the associated compression in the absence of electrochemical processes did not damage the ice-templated anode. Figure 3D,F show SEM images of microstructure of LTO anode after a single cycle and four cycles, respectively. Following electrochemical cycling and removal from a flat cell, electrodes were also visually observed macroscopically to be physically intact. SEM images did not reveal any noticeable difference between microstructures prior to and after electrochemical cycling. Overall, the ice-templated-sintered LTO anodes appeared physically intact and damage-free even after completion of four electrochemical cycles and the associated intercalation and deintercalation of Li^+ from the crystal structure.

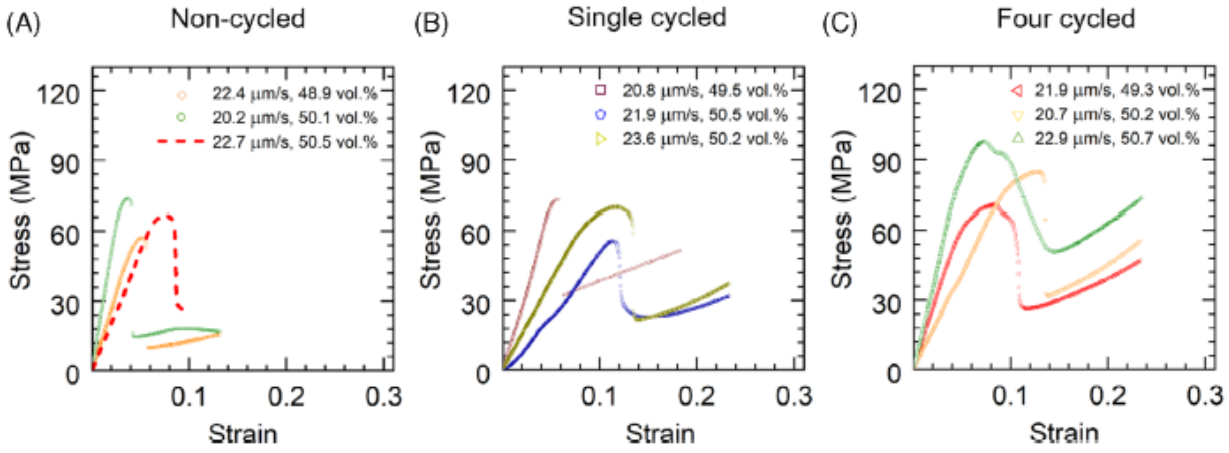

FIGURE 4 Stress–strain curves of (A) noncycled, (B) single-cycled, and (C) four-cycled lithium titanate (LTO) anodes, respectively. The curve in (A) with a red dashed line shows the compressive response of LTO anode assembled into the flat cell and removed without cycling. For each LTO anode, freezing front velocity (FFV) and porosity values are provided in the figure

3.3 | Uniaxial compressive mechanical response of LTO anodes

Figure 4A-C show uniaxial compressive response of the ice-templated-sintered LTO electrode pellets as prepared without cycling, after a single charge/discharge cycle, and after four charge/discharge cycles, respectively. For each specimen, FFV and porosity values have been indicated in the figures. In Figure 4A, stress–strain data for one LTO sample (red dashed curve) corresponds to where the anode was assembled in a flat cell but removed without any electrochemical cycling. All the samples exhibited similar compressive response, where stress increased linearly with strain in the elastic regime. After reaching maximum stress (peak stress, σ_p), all the samples exhibited catastrophic-type failure characterized by an abrupt drop in stress. Noncycled and single-cycled LTO anodes exhibited σ_p of 65.7 ± 6.8 MPa and 66.2 ± 7.5 MPa, respectively. Error represents the SD of 3 independent samples. No statistically significant difference was noticed between the strength of noncycled and single-cycled samples as the P-value was .94 (ie, $P > .05$). The LTO electrodes which experienced four charge/discharge cycles exhibited slightly higher strength with σ_p of 85.8 ± 7.8 MPa. Error represents the SD of 3 independent samples. The P-value between the strength of noncycled and four-cycled samples was 0.03 (ie, $P < .05$), which indicated statistically significant difference in strength. Higher strength for the LTO anodes cycled four times relative to the other electrodes was attributed to microstructure variation across the batches, which has been previously reported in ice-templating processes.[48] Ice-templated microstructure for four-cycled LTO anodes was observed to be relatively more dendritic due to higher density of lamellar bridges (Figure 3E,F) compared to the other LTO materials (Figure 3A-D). With increased dendritic morphology, ice-templated-sintered LTO materials have been reported to exhibit increased uniaxial compressive strength.[36] The most important result from Figure 4 was that ice-templated-sintered LTO anodes were physically and mechanically intact even after multiple cycles of electrochemical charge/discharge and associated intercalation and deintercalation of large amounts of lithium from the solid phase. The sintered electrodes sustained any stresses resulting from assembly and electrochemical cycling and maintained compressive load-bearing capacity. Microstructure analysis indicated structural integrity of ice-templated LTO electrodes, and compression tests revealed that ice-templated pore architecture was indeed mechanically robust for the anode material and conditions evaluated. While a comparison of compressive strength of nontemplated- and templated-sintered LTO electrodes is beyond the scope of this study, the current results are encouraging for realizing the multifunctional benefits of ice-templated electrodes in LIBs.

The structural stability of the LTO anode material was attributed in part to the negligible volume change (~0.2%) during intercalation and deintercalation.[49] As mentioned before, LTO has been reported as a zero-strain or minimal strain material for LIBs.[37] On the contrary, the sintered LCO materials were qualitatively not as structurally stable. While opening the flat cell after cycling, the LCO pellets would often crack into smaller pellets, indicating that the volume change (~1.9%) during intercalation and deintercalation may have resulted in high internal stress which broke the pellets.[6] It is noted that the LCO was not as sintered as the LTO and was a thinner electrode, which may have impacted its relative structural stability and/or compressive strength.

Fortunately, cracks in the LCO were observed in the direction perpendicular to the current collector and the carbon paste, which attached the LCO to the current collector and held the electrode in place. Thus, the LTO/LCO cells with sintered electrodes could still be cycled, and in coin cell configurations have successfully been cycled many times. For example, in a prior report, the capacity retention was still above 90% after cycling at C/20 for 100 cycles in coin cells with LTO and LCO-sintered electrodes.[15]

3.4 | Future considerations

As described above, for the electrochemical cycling conducted with the electrodes in this study, LTO was able to retain its mechanical strength in an all active material ice-templated electrode. However, due to experimental limitations of the use of such thick electrodes (even for sintered electrode systems), the cycling conditions were constrained. Future directions would include conducting more extensive cycling. For example, increasing the cycling to achieve hundreds of cycles which have previously been achieved with sintered LTO electrodes, such that it can be investigated what impacts extended cycling and fatigue have on the LTO materials. This will require investigating suitable mechanical compression systems which can accommodate thinner electrodes (eg, 1 mm or less thickness samples rather than 2 mm thick). At lower thicknesses, the impact of different rates of electrochemical cycling, and consequently different rates of strain applied, would also be accessible for study. Lower thickness will also facilitate more conventional cell components, which can be more reliably sealed and avoid the electrolyte evaporation challenges experienced herein. Also, while the LTO was intact, the LCO cathode was always cracked after cycling. This result may suggest that the strain experienced by LCO was sufficient to result in cracking the electrode, though it is noted that processing of the LCO was quite different than the LTO with regards to thickness and thermal treatment. Similar cracking phenomena may also occur with other battery materials such as $LiFePO_4$ or $LiMn_2O_4$, as they also undergo increased volume change during cycling relative to LTO.[6] Finding additional "zero-strain" materials for sintered electrodes is challenging, as there are many properties necessary for a successful electrode material in addition to minimizing volume change (eg, ionic/electronic conductivity and electrochemical potential). However, more systematic investigation of the strain that can be accommodated without cracking would provide metrics for the design limits that result in robust sintered electrodes. Finally, this study investigated how electrochemical cycling influenced compressive strength, but another consideration is how compression influences the electrochemical properties. Some materials have been reported to have electrochemical properties, which are sensitive to applied pressure.[50] An unexplored area for these sintered electrodes is whether varying the compressive forces influences the electrochemical properties of the material with all other physical properties kept nominally equivalent in the cell.

4 | CONCLUSIONS

This study investigated the electrochemical and mechanical properties of ice-templated-sintered LTO anodes. Sintered electrodes can be fabricated with very large thicknesses, which can result in increased energy densities at the cell level. However, the sintered electrodes must have multifunctional properties of providing electrochemical capacity and accepting the compressive stresses of cell fabrication. This was the first report to the authors' knowledge on the mechanical properties of ice-templated-sintered electrodes before and after electrochemical cycling. For the ice-templated LTO anodes, the microstructure and compressive strength were retained with cycling and not significantly changed relative to the nominally identical materials that were not cycled. These results suggest that at least for LTO, which has very minimal strain experienced during electrochemical cycling, that multifunctional mechanical and electrochemical properties of ice-templated electrodes may be retained with multiple cycles.

ACKNOWLEDGMENTS

This research was supported by the National Science Foundation via grant CMMI-1825216.

DATA AVAILABILITY STATEMENT

The data that support the findings will be available in Libra at https://www.library.virginia.edu/libra/ following an embargo from the date of publication to allow for commercialization of research findings.

ORCID

Gary M. Koenig Jr https://orcid.org/0000-0002-7172-7819

REFERENCES

1. Nie Z, Parai R, Cai C, et al. Pore microstructure impacts on lithium-ion transport and rate capability of thick sintered electrodes. *J Electrochem Soc*. 2021;168:060550.

2. Chen Z, Dahn JR. Reducing carbon in $LiFePO_4$/C composite electrodes to maximize specific energy, volumetric energy, and tap density. *J Electrochem Soc*. 2002;149:A1184-A1189.
3. Mistry A, Trask S, Dunlop A, et al. Quantifying negative effects of carbon-binder networks from electrochemical performance of porous Li-ion electrodes. *J Electrochem Soc*. 2021;168:070536.
4. Boz B, Dev T, Salvadori A, Schaefer JL. Review—Electrolyte and electrode designs for enhanced ion transport properties to enable high performance lithium batteries. *J Electrochem Soc*. 2021;168:090501.
5. Robinson JP, Ruppert JJ, Dong H, Koenig GM Jr. Sintered electrode full cells for high energy density lithium-ion batteries. *J Appl Electrochem*. 2018;48:1297-1304.
6. Lai W, Erdonmez CK, Marinis TF, et al. Ultrahigh-energy-density microbatteries enabled by new electrode architecture and micro packaging design. *Adv Energy Mater*. 2010;22:E139-E144.
7. Sotomayor ME, de La Torre-Gamarra C, Levenfeld B, et al. Ultra-thick battery electrodes for high gravimetric and volumetric energy density Li-ion batteries. *J Power Sources*. 2019;437:226923.
8. Nie Z, Ong S, Hussey DS, LaManna JM, Jacobson DL. Probing transport limitations in thick sintered battery electrodes with neutron imaging. *Mol Syst Des Eng*. 2020;5:245-256.
9. Wu J, Ju Z, Zhang X, et al. Ultrahigh-capacity and scalable architected battery electrodes via tortuosity modulation. *ACS Nano*. 2021;15:19109-19118.
10. Wu J, Ju Z, Zhang X, et al. Building efficient ion pathway in highly densified thick electrodes with high gravimetric and volumetric energy densities. *Nano Lett*. 2021;21:9339-9346.
11. Gallagher KG, Trask SE, Bauer C, et al. Optimizing areal capacities through understanding the limitations of lithium-ion electrodes. *J Electrochem Soc*. 2015;163:A138-A149.
12. Wu J, Zhang X, Ju Z, et al. From fundamental understanding to engineering design of high-performance thick electrodes for scalable energy-storage systems. *Adv Mater*. 2021;33:2101275.
13. Wood M, Li J, Du Z, et al. Impact of secondary particle size and two-layer architectures on the high-rate performance of thick electrodes in lithium-ion battery pouch cells. *J Power Sources*. 2021;515:230429.
14. Cai C, Koenig GM Jr. Investigating dopants to improve sintered $LiMn_2O_4$ spinel electrode electrochemical cycling limitations. *Electrochim Acta*. 2022;401:139484.
15. Nie Z, Parai R, Chen C, Ghosh D, Koenig GM Jr. Improving high rate cycling limitations of thick sintered battery electrodes by mitigating molecular transport limitations through modifying electrode microstructure and electrolyte conductivity. *Mol Syst Des Eng*. 2021;6:708-712.
16. Cai C, Nie Z, Robinson JP, et al. Thick sintered electrode lithium-ion battery discharge simulations: incorporating lithiation-dependent electronic conductivity and lithiation gradient due to charge cycle. *J Electrochem Soc*. 2020;167:140542.
17. Nie Z, McCormack P, Bilheux HZ, et al. Probing lithiation and delithiation of thick sintered lithium-ion battery electrodes with neutron imaging. *J Power Sources*. 2019;419:127-136.
18. Tambio SJ, Cadiou F, Maire E, Besnard N, Deschamps M, Lestriez B. The concept of effective porosity in the discharge rate performance of high-density positive electrodes for automotive application. *J Electrochem Soc*. 2020;167:160509.
19. Alcaide F, Delacourt C, Urdampilleta I, Vicedo R, Ayerbe E. New insights on tortuosity determination by eis for battery electrodes: effect of electrolyte concentration and temperature. *J Electrochem Soc*. 2021;168:110514.
20. Kim W, Jang D, Kim HJ. Understanding electronic and Li-ion transport of $LiNi_{0.5}Co_{0.2}Mn_{0.3}O_2$ electrodes affected by porosity and electrolytes using electrochemical impedance spectroscopy. *J Power Sources*. 2021;510:230338.
21. Diercks DR, Musselman M, Morgenstern A, et al. Evidence for anisotropic mechanical behavior and nanoscale chemical heterogeneity in cycled $LiCoO_2$. *J Electrochem Soc*. 2014;161:F3039-F3045.
22. Gunther T, Schreiner D, Metkar A, Meyer C, Kwade A, Reinhart G. Classification of calendering-induced electrode defects and their influence on subsequent processes of lithium-ion battery production. *Energ Technol*. 2019;8:1900026.
23. Singh M, Kaiser J, Hahn H. Thick electrodes for high energy lithium-ion batteries. *J Electrochem Soc*. 2015;162:A1196-A1201.
24. Ryu HH, Namkoong B, Kim JH, Belharouak I, Yoon CS, Sun YK. Capacity fading mechanisms in Ni-rich single-crystal ncm cathodes. *ACS Energy Lett*. 2021;6:2726-2734.
25. Tariq F, Yufit V, Eastwood DS, et al. In-operando X-ray tomography study of lithiation induced delamination of Si based anodes for lithium-ion batteries. *ECS Electrochem Lett*. 2014;3:A76-A78.
26. Hodson T, Patil S, Steingart DA. An initial exploration of coupled transient mechanical and electrochemical behaviors in lithium-ion batteries. *J Electrochem Soc*. 2021;168:070515.
27. Zhou T, Dickinson E, Boyd JG, Lutkenhaus J, Lagoudas DC. Multifunctional efficiency metric for structural supercapacitors. *Multifunct Mater*. 2020;3:044002.
28. Mullenax J, Browning P, Huebsch W, Gautam M, Sabolsky EM. Composite multifunctional lithium-ion batteries. *ECS Trans*. 2012;41:175-185.
29. Thomas JP, Qidwai SM, Pogue WR III, Pham GT. Multifunctional structure-battery composites for marine systems. *J Compos Mater*. 2012;47:5-26.
30. Antartis D, Dillon S, Chasiotis I. Effect of porosity on electrochemical and mechanical properties of composite Li-ion anodes. *J Compos Mater*. 2015;49:1849-1862.
31. Bruggeman DAG. Berechnung verschiedener physikalischer konstanten von heterogenen substanzen. I. dielektrizitatskonstanten und leitfahigkeiten der mischkorper aus isotropen substanzen. *Ann Phys*. 1935;416:636-664.
32. Ebner M, Marone F, Stampanoni M, Wood V. Visualization and quantification of electrochemical and mechanical degradation in Li-ion batteries. *Science*. 2013;342:716-720.
33. Thorat IV, Stephenson DE, Zacharias NA, Zaghib K, Harb JN, Wheeler DR. Quantifying tortuosity in porous Li-ion battery materials. *J Power Sources*. 2009;188:592-600.
34. Delattre B, Amin R, Sander J, Coninck JD, Tomsia A, Chiang YM. Impact of pore tortuosity on electrode kinetics in lithium battery electrodes: study in directionally freeze-cast $LiNi_{0.8}Ca_{0.15}Al_{0.05}O_2$ (NCA). *J Electrochem Soc*. 2018;165:A388-A395.
35. Huang C, Grant P. Coral-like directional porosity lithium-ion battery cathodes by ice templating. *J Mater Chem A*. 2018;6:14689-14699.

36. Parai R, Walters T, Marin J, Pagola S, Koenig GM Jr, Ghosh D. Strength enhancement in ice-templated lithium titanate $Li_4Ti_5O_{12}$ materials using sucrose. *Materialia*. 2020;14:100901.
37. Sun X, Radovanovic PV, Cui B. Advances in spinel $Li_4Ti_5O_{12}$ anode materials for lithium-ion batteries. *New J Chem*. 2015;39:36-63.
38. Deville S, Saiz E, Nalla RK, Tomsia AP. Freezing as a path to build complex composites. *Science*. 2006;311:515-518.
39. Ghosh D, Kang H, Banda M, Kamaha V. Influence of anisotropic grains (platelets) io the microstructure and uniaxial compressive response of ice-templated sintred alumina scaffolds. *Acta Mater*. 2017;125:1-14.
40. Ghosh D, Dhavale N, Bamda M, Kang H. A comparison of microstructure and uniaxial compressive response of ice-templated alumina scaffolds fabricated from two different particle sizes. *Ceram Int*. 2016;42:16138-16147.
41. Munch E, Saiz E, Tomsia AP, Deville S. Architectural control of freeze-cast ceramics through additives and templating. *J Am Ceram Soc*. 2009;92:1534-1539.
42. Frank MB, Siu SH, Karandikar K, et al. Synergistic structures from magnetic freeze casting with surface magnetized alumina particles and platelets. *J Mech Behav Biomed Mater*. 2017;76:153-163.
43. Akurati S, Qian S, Ghosh D. AC electric field assisted fabrication of ice-templated alumina materials and remarkable enhancement of compressive strength. *Scr Mater*. 2022;206:114264.
44. Ohzuku T, Ueda A, Yamamoto N. Zero-strain insertion material of Li $[Li_{1/3}Ti_{5/3}]O_4$ for rechargeable lithium cells. *J Electrochem Soc*. 1995;142:1431-1435.
45. Qi Z, Koenig GM Jr. High-performance $LiCoO_2$ submicrometer materials from scalable microparticle template processing. *ChemistrySelect*. 2016;1:3992-3999.
46. Qi Z, Koenig GM Jr. A carbon-free lithium-ion solid dispersion redox couple with low viscosity for redox flow batteries. *J Power Sources*. 2016;323:97-106.
47. Dhavale ND. A Comparison of Microstructure and Uniaxial Compressive Response of Ice-Templated Porous Alumina Scaffolds Fabricated from Two Different Particle Sizes. [master's thesis]. Norfolk, VA: Old Dominion University; 2016.
48. Naleway SE, Fickas KC, Maker YN, Meyers MA, McKittrick J. Reproducibility of ZrO_2-based freeze casting of biomaterials. *Mater Sci Eng C*. 2016;61:105-112.
49. Nitta N, Wu F, Lee JT, Yushin G. Li-ion battery materials: present and future. *Mater Today*. 2015;18:252-264.
50. Madsen KE, Shin M, Gewirth AA. Pressure-dependent electrochemical behavior of di-lithium rhodizonate cathodes. *Chem Mater*. 2021;33:5738-5747.

SUPPORTING INFORMATION

Additional supporting information may be found in the online version of the article at the publisher's website.

How to cite this article: Parai R, Nie Z, Ghosh D, Koenig GM Jr. Microstructure and mechanical properties of electrochemically cycled ice-templated $Li_4Ti_5O_{12}$ sintered anodes. *Int J Energy Res*. 2022;46(8):11501-11509. doi:10.1002/er.7909